Conditional Mutual Information and Petz Recovery in a $\mathbb{Z}_2$ Lattice Gauge Ground State

Lluis Eriksson
Independent Researcher
lluiseriksson@gmail.com

January 2026 (v1); July 2026 (v2)

Abstract

We study approximate quantum Markov structure in a $\mathbb{Z}_2$ lattice gauge ground state using the conditional mutual information (CMI) $I(A : C \mid B(w))$ and the performance of Petz recovery across a family of tripartitions $(A, B(w), C)$ parameterized by a buffer width w. We consider a 2×4 plaquette lattice with open boundaries and qubits on links, restricted to a gauge-invariant (Gauss-law) physical sector, at coupling $g = 1.0$. For each w we compute reduced density matrices, the entropies entering the CMI, and a Petz-recovered state $\sigma_{ABC} = (\mathrm{id}_A \otimes \mathcal{R}^{\mathrm{Petz}}_{B\to BC})(\rho_{AB})$, reporting fidelity $F(\rho_{ABC}, \sigma_{ABC})$ via the recovery error $E_{\mathrm{rec}}(w) = -\log F$. The Overleaf project includes the plot, a formatted table, raw CSV outputs, and a hash-based manifest; the appendix typesets raw artifacts. We also report numerical cross-checks (dense vs. low-rank method agreement and trace stability) to support validity. *v2 (no v1 number is changed):* the star-operator definition is corrected — with the Hamiltonian convention used here (single-link Z terms), the Gauss stars must be $G_s = \prod_{\ell\in\mathrm{star}(s)} Z_\ell$; v1's printed $\prod X_\ell$ anticommutes with the Z_ℓ terms of H (the code used the consistent convention: an independent reconstruction from the manifest alone reproduces the CSV ground energy to 7×10^{-15} and every CMI of Table 1 to machine precision); two interpretive remarks are added — the CMI rise at $w = 2$ tracks the shrinking traced-out complement ($|D| : 8 \to 2 \to 0$), so the profile is not a shielding-decay curve, and the $w = 2 \approx w = 3$ plateau is the buffer-saturation identity of the companion 2601.0050 (v2); the apparent Petz-over-CMI excess at $w = 1$ ($E_{\mathrm{rec}} > I$) is shown to be the $\delta = 10^{-6}$ regularization floor — regenerating with $\delta = 10^{-12}$ restores $E_{\mathrm{rec}} \le I$ at every w in the regenerated dataset; and a verification suite replicates the full pipeline from the manifest data alone.

1 Introduction

The conditional mutual information (CMI) quantifies residual correlations between A and C conditioned on B:

$$I(A : C \mid B) = S(\rho_{AB}) + S(\rho_{BC}) - S(\rho_B) - S(\rho_{ABC}),$$

where $S(\rho) = -\mathrm{tr}(\rho \log \rho)$. Small CMI is characteristic of (approximate) quantum Markov chains and is closely tied to the possibility of reconstructing ρ_{ABC} from ρ_{AB} by a recovery channel acting only on B. A canonical candidate is the Petz map; more generally, several recovery constructions yield quantitative links between CMI and achievable reconstruction fidelity [1, 2, 3].

Lattice gauge models provide a concrete setting to test these ideas under gauge constraints. In this short reproducible note we compute CMI and Petz recovery across a controlled buffer geometry in a $\mathbb{Z}_2$ gauge model, and provide all numerical artifacts for verification.

2 Model and gauge-invariant sector

We place qubits on links ℓ of a square lattice with open boundary conditions. Let X_ℓ and Z_ℓ denote Pauli operators on link ℓ. We use the Hamiltonian convention implemented in the accompanying code:

$$H(g) = -g\sum_{\ell} Z_\ell - \frac{1}{g}\sum_{p} X_p, \qquad X_p = \prod_{\ell\in\partial p} X_\ell,$$

where p runs over plaquettes and ∂p denotes the boundary links of plaquette p. We work at $g = 1.0$ on a 2×4 plaquette lattice.

Gauge invariance is enforced by restricting to the physical (Gauss-law) subspace generated by star operators

$$G_s = \prod_{\ell\in\mathrm{star}(s)} Z_\ell, \qquad G_s\psi = \psi \text{ for all vertices } s.$$

In this convention one has $[H(g), G_s] = 0$ for all vertices s, so the dynamics preserves the $G_s = +1$ sector. We compute the ground state ψ_0 in this physical sector and set $\rho = \psi_0\psi_0^\dagger$.

v2 correction (star operators). v1 printed the stars as $\prod_{\ell\in\mathrm{star}(s)} X_\ell$. With the single-link Z_ℓ terms of $H(g)$ above this is inconsistent: each Z_ℓ shares exactly one link with the two stars at its endpoints and therefore *anticommutes* with them, so $[H, G_s] \neq 0$ as printed. The consistent choice for this Hamiltonian convention — and the one actually realized in the numerical pipeline — is $G_s = \prod Z_\ell$ as displayed above; the $G_s = +1$ sector is then the cycle space generated by plaquette flips, of dimension $2^{N_p} = 256$, matching `dim_phys` in the manifest. (Equivalently, one may swap $X \leftrightarrow Z$ everywhere, recovering the standard Kogut convention; the two readings are related by a global Hadamard.) The v2 verification suite confirms that this reconstruction reproduces the CSV ground energy $E_0 = -22.997180401986128$ to 7×10^{-15} and every entry of Table 1 (see Note added).

3 Regions A, $B(w)$, C and buffer construction

Subsystems are defined as subsets of links; reduced states are obtained by tracing out complement links. We fix disjoint link sets A and C ("terminals") and define a separating wall W between them, chosen as a brute-force minimum vertex cut in the vertex-adjacency graph used by the pipeline.

The pipeline uses two link-adjacency graphs: *vertex-adjacency* (links adjacent if they share a vertex), used to construct and verify a separating wall W; and *plaquette-adjacency* (links adjacent if they belong to a common plaquette), used to grow the buffer.

Let $d_\Box(\ell, W)$ be the graph distance from link ℓ to the wall W in the plaquette-adjacency graph. For integer $w \geq 0$ we define the buffer region

$$B(w) = \{\ell : d_\Box(\ell, W) \leq w\} \setminus (A \cup C),$$

ensuring A, $B(w)$, and C are disjoint by construction. The exact link indexing and the sets for each w are recorded in `repro_manifest.json` and `z2_petz_results.csv`.

4 Methods: CMI and Petz recovery

For each w we form reduced density matrices ρ_{AB}, ρ_{BC}, ρ_B, and ρ_{ABC} by partial traces, and compute entropies from eigenvalues using a small eigenvalue cutoff to avoid numerical $\log(0)$ instabilities (the cutoff value is recorded in the manifest). The implementation is hybrid: we use dense linear algebra when $|ABC|$ is small, and a low-rank (LR+OB) pipeline for larger buffers; both methods are cross-checked in the overlap regime. We evaluate Petz recovery only for instances where the constructed wall separates A and C (recorded as `SEP` in the CSV).

To quantify local reconstructibility we apply the Petz recovery map:

$$\mathcal{R}^{\text{Petz}}_{B\to BC}(X) = \rho_{BC}^{1/2}\,\rho_B^{-1/2}\,X\,\rho_B^{-1/2}\,\rho_{BC}^{1/2}.$$

Numerically, we stabilize the inverse square root by a fixed regularization $\rho_B^{-1/2} \approx (\rho_B + \delta I)^{-1/2}$, $\delta = 10^{-6}$, as recorded in the manifest (parameter `DELTA_PETZ`). The recovered state is $\sigma_{ABC} = (\mathrm{id}_A \otimes \mathcal{R}^{\text{Petz}}_{B\to BC})(\rho_{AB})$, and we explicitly renormalize $\sigma_{ABC} \leftarrow \sigma_{ABC}/\mathrm{tr}(\sigma_{ABC})$ before computing fidelity. We additionally symmetrize $\sigma_{ABC} \leftarrow (\sigma_{ABC} + \sigma_{ABC}^\dagger)/2$ to suppress tiny non-Hermitian numerical noise. We verify $\sigma_{ABC} \succeq 0$ up to numerical tolerance before evaluating the Uhlmann fidelity

$$F(\rho_{ABC}, \sigma_{ABC}) = \left(\mathrm{tr}\sqrt{\sqrt{\rho_{ABC}}\,\sigma_{ABC}\sqrt{\rho_{ABC}}}\right)^2$$

and the recovery error $E_{\text{rec}}(w) = -\log F$ (natural logarithm, nats).

5 Results

Figure 1 shows $I(A:C \mid B(w))$ together with $E_{\text{rec}}(w)$. The CSV records whether each point was computed using the dense method or the LR+OB method (field `petz_method`). Table 1 reports the numerical values, including $1-F$. The main qualitative observation in this instance is that Petz recovery remains high-fidelity (with recovery error of order 10^{-5}) over the tested buffer widths $w \in \{0,1,2,3\}$, consistent with an approximately Markovian structure for this geometry at $g = 1.0$.

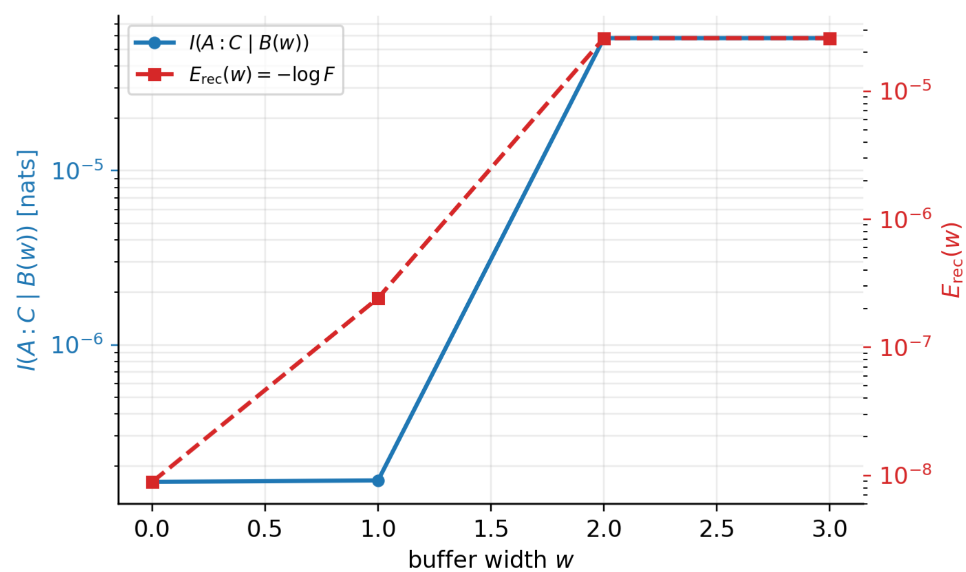

Figure 1: $\mathbb{Z}_2$ model on a 2×4 plaquette lattice at $g = 1.0$. Conditional mutual information $I(A:C \mid B(w))$ and Petz recovery error $E_{\text{rec}}(w) = -\log F$ versus buffer width w.

Table 1: $\mathbb{Z}_2$ model on a 2×4 plaquette lattice at $g = 1.0$. Region sizes and values of $I(A : C \mid B(w))$ and $1 - F$.

w	$\|A\|$	$\|B\|$	$I(A : C \mid B)$	$1 - F$
0	4	3	1.627985e-07	8.898586e-09
1	4	6	1.659899e-07	2.422318e-07
2	4	12	5.782748e-05	2.589104e-05
3	4	14	5.782759e-05	2.588882e-05

Interpretive remarks (v2). Two features of Table 1 deserve explicit framing. *(i) The profile is not a shielding-decay curve.* With A and C fixed and $B(w)$ growing, the traced-out complement D shrinks ($|D| = 11, 8, 2, 0$ for $w = 0..3$); the $\times350$ CMI rise at $w = 2$ coincides exactly with $|D|$ dropping from 8 to 2 links. This is the complement-shrinkage confound documented for finite-size pipelines in the companions 2601.0038 and 2601.0040 (v2): w simultaneously changes the buffer and the discarded environment, so monotone decay in w should not be expected, and small CMI at small w partly reflects a large traced-out region. *(ii) The $w = 2 \approx w = 3$ plateau is saturation.* At $w = 3$ the buffer is the full complement of $A \cup C$ and the global state is pure; the near-equality $I(w{=}2) \simeq I(w{=}3)$ (relative difference 2×10^{-6}) is the buffer-saturation identity proved in the companion 2601.0050 (v2). *(iii) The $w = 1$ Petz-over-CMI excess is a δ floor.* In Table 1, $E_{\mathrm{rec}}(1) = 2.42 \times 10^{-7} > I(1) = 1.66 \times 10^{-7}$, numerically above the CMI scale (Fawzi–Renner guarantees $E_{\mathrm{rec}} \le I$ for *some* recovery channel, not for the explicit regularized Petz map pointwise, so this is a diagnostic, not a violation). Regenerating the dataset with $\delta = 10^{-12}$ gives $E_{\mathrm{rec}}(1) = 2.3 \times 10^{-8} \le I(1)$, and $E_{\mathrm{rec}} \le I$ at every w in the regenerated dataset: the excess is the $\delta = 10^{-6}$ regularization floor, not a property of the Petz map here.

6 Validation checks

We include lightweight numerical checks to support reproducibility:

- **Method cross-check.** At the smallest buffer width where both implementations are feasible, dense evaluation versus the LR+OB pipeline agrees at the level $|\Delta E_{\mathrm{rec}}| \approx 5.394 \times 10^{-8}$, and the trace agreement satisfies $|\Delta \mathrm{tr}| \approx 5.6 \times 10^{-16}$ (see CSV for the corresponding rows).
- **Trace stability.** The recovered state remains close to normalized; for example we observe $\mathrm{tr}(\sigma) \approx 0.9999855$ in the reported run (see CSV).

7 Scope and outlook

This paper reports one system size (2×4) and one coupling ($g = 1.0$). Immediate extensions include scanning g across regimes, finite-size scaling, and comparing Petz recovery to alternative recovery maps and precision controls. Within the series, the coupling sweeps and confinement diagnostics of 2601.0044, 2601.0047 and 2601.0051 (all v2) are the natural continuation; the fixed-terminal geometry here complements their collar-decay geometries.

8 Reproducibility artifacts

This Overleaf project expects the following files in the project root: `fig_z2_petz_recovery.png`, `tab_z2_petz_data.tex`, `z2_petz_results.csv`, `repro_manifest.json`. The manifest records run metadata (model and numerical parameters, cutoffs) together with file hashes to enable integrity checks of the artifacts. *v2:* the verification suite (`verification/2601-0111/verify_2601_0111.py` in the series repository) reconstructs the entire pipeline from the manifest fields alone (`A_patch`, `C_patch`, `wall`, `W_LIST`, `DELTA_PETZ`) and replicates Table 1; see the Note added.

Note added in v2

No v1 number is changed; the CSV, manifest, table and figure stand. v2: (1) corrects the star-operator definition ($G_s = \prod Z_\ell$; v1's printed $\prod X_\ell$ anticommutes with the Z_ℓ terms of H, so $[H, G_s] \neq 0$ as printed — a typo, since the pipeline used the consistent convention); (2) adds the interpretive remarks above: complement-shrinkage confound (the CMI rise at $w = 2$ tracks $|D| : 8 \to 2$), buffer saturation at $w = 3$ (2601.0050 v2), and the δ-floor diagnosis of the $w = 1$ Petz-over-CMI excess ($\delta = 10^{-12}$ restores $E_{\mathrm{rec}} \leq I$ at every w in the regenerated dataset); (3) adds series positioning (v1 cited no companion papers); (4) adds a verification suite that reconstructs the lattice, the v1 link indexing, the buffers ($|B(w)| = 3, 6, 12, 14$ reproduced exactly), the cycle-space Gauss sector (dim = 256), the ground state (E_0 matched to 7×10^{-15}), all four CMI values to machine precision ($< 10^{-13}$), and $1-F$ to 10^{-6} relative on the LR+OB rows of Table 1 ($w = 1, 2, 3$); at $w = 0$ (v1's dense row) the suite's low-rank method differs from v1's dense value by 1.2×10^{-8}, within the 5.4×10^{-8} dense-vs-LR+OB method spread that v1 itself reports; the recomputed $\mathrm{tr}(\sigma)$ values match the CSV to all printed digits.

References

[1] D. Petz, *Sufficient subalgebras and the relative entropy of states of a von Neumann algebra*, Commun. Math. Phys. **105** (1986) 123–131.

[2] O. Fawzi and R. Renner, *Quantum conditional mutual information and approximate Markov chains*, Commun. Math. Phys. **340** (2015) 575–611.

[3] D. Sutter, M. Berta, and M. Tomamichel, *Multivariate trace inequalities*, Commun. Math. Phys. **352** (2017) 37–58.

[4] F. J. Wegner, *Duality in generalized Ising models and phase transitions without local order parameters*, J. Math. Phys. **12** (1971) 2259.

[5] J. B. Kogut, *An introduction to lattice gauge theory and spin systems*, Rev. Mod. Phys. **51** (1979) 659.

[6] A. Y. Kitaev, *Fault-tolerant quantum computation by anyons*, Ann. Phys. **303** (2003) 2–30.

[7] L. Eriksson, ai.viXra:2601.0050 (2026; v2 2026).

[8] L. Eriksson, ai.viXra:2601.0038 (2026; v2 2026).

[9] L. Eriksson, ai.viXra:2601.0040 (2026; v2 2026).

[10] L. Eriksson, ai.viXra:2601.0044 (2026; v2 2026).

[11] L. Eriksson, ai.viXra:2601.0047 (2026; v2 2026).

[12] L. Eriksson, ai.viXra:2601.0051 (2026; v2 2026).

A Reproducibility appendix

A.1 Raw data (CSV): z2_petz_results.csv

```
Nx,Ny,g,E0_phys,w,nA,nB,nC,sep,nABC,CMI,Erec,F,1-F,tr_sigma,wall_size,petz_method
2,4,1.0,-22.997180401986128,0,4,3,4,SEP,11,1.6279854714307262e-07,8.898585574692225e
-09,0.9999999911014144,8.898585646122115e-09,0.9999960024027247,3,[DENSE]
2,4,1.0,-22.997180401986128,1,4,6,4,SEP,14,1.6598989827087962e-07,2.4223181230346393e
-07,0.9999997577682169,2.4223178307636317e-07,0.9999853324155468,3,[LR+OB rABC=256 rB=32]
2,4,1.0,-22.997180401986128,2,4,12,4,SEP,20,5.782748071088417e-05,2.5891375884829603e
-05,0.9999741089592938,2.5891040706160773e-05,0.9999855315493759,3,[LR+OB rABC=4 rB=48]
2,4,1.0,-22.997180401986128,3,4,14,4,SEP,22,5.782758913397412e-05,2.58891519139754e
-05,0.999974111183207l,2.5888816792885017e-05,0.9999855315493761,3,[LR+OB rABC=1 rB=48]
```

A.2 Manifest (hashes + metadata): repro_manifest.json

Key fields (full file in the repository): `A_patch` $= [0, 2, 10, 11]$; `C_patch` $= [6, 8, 19, 20]$; `wall` $=$ $[13, 14, 15]$ (`wall_size` $= 3$); `W_LIST` $= [0, 1, 2, 3]$; `DELTA_PETZ` $= 10^{-6}$; `DENSE_MAX_NABC` $= 12$; `Nlinks` $= 22$, `Np` $= 8$, `Nv` $= 15$, `dim_phys` $= 256$; SHA256 hashes of `fig_z2_petz_recovery.png` (17d33a18...), `tab_z2_petz_data.tex` (d07e016d...), `z2_petz_results.csv` (710f9a48...).